Natural hydrogel in American lobster: A soft armor with high toughness and strength

Citation: Wu, Jinrong et al. "Natural hydrogel in American lobster: A soft armor with high toughness and strength." Acta Biomaterialia 88 (April 2019): 102-110 © 2019 Acta Materialia Inc

As Published: http://dx.doi.org/10.1016/j.actbio.2019.01.067

Publisher: Elsevier BV

Persistent URL: https://hdl.handle.net/1721.1/127837

Version: Author's final manuscript: final author's manuscript post peer review, without publisher's formatting or copy editing

Natural hydrogel in American lobster: a soft armor with high toughness and strength

Jinrong Wu[a], Zhao Qin[b]*, Liangliang Qu[c], Hao Zhang[a], Fei Deng[c], Ming Guo[d]*

Affiliations

[a]State Key Laboratory of Polymer Materials Engineering, College of Polymer Science and Engineering, Sichuan University, Chengdu, 610065, China;

[b]Department of Civil and Environmental Engineering, Massachusetts Institute of Technology, Cambridge, MA 02139, USA;

[c]John A. Paulson School of Engineering and Applied Sciences, Harvard University, Cambridge, MA 02138, USA;

[d]Department of Mechanical Engineering, Massachusetts Institute of Technology, Cambridge, MA 02139, USA;

***Correspondence**:

Ming Guo. Email: guom@mit.edu

Zhao Qin. Email: qinzhao@mit.edu

Submitted to: *Acta Biomaterialia*

Abstract

The *Homarus americanus*, known as American lobster, is fully covered by its exoskeleton composed of rigid cuticles and soft membranes. These soft membranes mainly locate at the joints and abdomen to connect the rigid cuticles, and greatly contribute to the agility of the lobster in swimming and preying. Here we show that the soft membrane from American lobster is a natural hydrogel (90% water) with exceptionally high toughness (14.02 MJ/m^3) and strength (17.91 MPa), and is very insensitive to cracks. By combining experimental measurements and large-scale computational modeling, we demonstrate that the unique multilayered structure in this membrane, achieved through the ordered arrangement of chitin fibers, plays a crucial role in dissipating energy during rupture, and making this membrane tough and damage-tolerant. The knowledge learned from the soft membrane of natural lobsters sheds light on designing synthetic soft, yet strong and tough materials for reliable usage under extreme mechanical conditions, including a flexible armor that can provide the full body protection without sacrificing limb mobility.

Keywords: American lobster; flexible body armor; hydrogel; multilayered structure; damage-tolerance.

1. Introduction

The exoskeleton of the *Homarus americanus*, known as American lobster[1], is composed of segments of hard cuticles connected by soft arthrodial membranes and acts as a barrier between the internal organs and the external environment. More importantly, it provides a protective armor against predatory attack, thus making the lobster one of the most successful species existing for more than 100 million years[1]. The hard cuticles are composed of the twisted plywood and the honeycomb-like structures, incorporating the biomineral nanoparticles for good hardness[2-4]. However, the soft membranes are quite different, as they have negligible amounts of calcification, a higher content of water and chitin, and different types of proteins as compared to the cuticles[2, 5]. Interestingly, these soft membranes cover a large portion of the lobster body, such as the abdomen, which is often subjected to wear and tear forces in sandy and rocky environments where lobsters typically live; this suggests that such soft membranes have a high mechanical reliability to protect the lobster tissue. Nevertheless, unlike the hard cuticles, the structure and mechanical function of the soft lobster membranes remain largely unknown, which may contain critical information to design a fully flexible body armor as well as other functional soft materials.

While ancient armors are designed to be stiff enough to resist deformation under external loading force, modern armors such as ballistic vest aim at stop and deform a bullet and spreading its force over a larger portion of the vest [6, 7]. It is more crucial to maximize the energy absorption during the penetration process than to completely prevent the deformation. Moreover, hard armors sacrifice limb mobility, which we believe is crucial when lobsters fight with each other to claim territory. Thus, we are interested in the protecting role of soft lobster membranes and study their capability of absorbing energy during the material fracture under loading.

Here we investigate the microstructure, mechanical properties and failure behavior of the lobster membranes and present our work in the following logic. We prepare samples of lobster membrane, visualize their microstructures and character their

mechanical properties. We build a large-scale coarse-grained model of the lobster membrane by following the geometric features as obtained from experimental images and mechanical measurement for chitin fibers and the lobster membrane. We thereafter use the model to simulate the mechanics of the cracked membrane in loading and obtain the membrane strength as a function of the crack depth. The experimental and modeling methods are summarized in session 2. In session 3, we summarize our key findings. Our results unravel that the lobster membranes are soft hydrogels containing 90% water; surprisingly, they exhibit extremely high toughness and tensile strength as well as a high tolerance to structural damages[8-10]. We find that these membranes are composed of highly ordered multi-layer structures at the microscopic level, which is common for mineralized natural materials[2, 6, 11-14] but rare for hydrogels. Our simulation based on the coarse-grained model reveals that this unique ordered structure strongly connects to the nonlinear mechanical and failure behaviors, which together give rise to the high toughness and damage-tolerance of the lobster membranes. In session 4, we provide our main conclusion of the work.

2. Methods

2.1. Experimental preparation of lobster membranes.

Joint and abdomen membranes are obtained from fresh American lobsters from Boston local fish markets. After carefully removing other attached tissues, the intact membranes are immersed in saline water with compositions similar to seawater (Na^+ 0.469 mol/kg, Mg^{2+} 0.053 mol/kg and Ca^{2+} 0.010 mol/kg) for 1 hour. Rectangular samples width from 2 to 5 mm, thickness from 0.3 to 0.5 mm, and length from 10 to 20 mm are cut from the membranes by a pair of sharp scissors for mechanical measurements. Mechanical properties are test within 24 h after sacrificing the animal.

2.2. Chemical characterization of lobster membranes and cuticles.

To confirm the chemical composition of the lobster membranes, Fourier transform infrared spectroscopy (FTIR) spectra are collected on a Perkin Elmer FTIR spectrometer fitted with an attenuated total reflectance cell.

2.3. X-Ray photoelectron spectroscopy (XPS).

Data are collected on a Thermo Scientific™ K-Alpha™+ XPS System with a monochromatic soft aluminum Kα X-ray generating 12 kV power, an energy of 1486.6 eV and a resolution of 0.3 eV. Samples are mounted by adhesion to double-sided electrically conducting tape, to minimize the charge effect on the samples. Analysis of the collected data is performed using the Thermo Scientific™ Avantage Software (Thermo Fisher Scientific, USA).

2.4. The SEM images for microstructure of lobster membranes

Images are obtained on the ZEISS Ultra55 Field Emission Scanning Electron Microscope at an acceleration voltage of 4kV after sputter-coating a Pt/Pd layer of 5nm in thickness. The cross-section of abdomen membrane is prepared by cutting liquid nitrogen frozen sample and then lyophilizing. EDX analysis is performed on a ZEISS Ultra55 Field Emission Scanning Electron Microscope with EDAX Genesis 2000 detector at an acceleration voltage of 8kV. The samples are vacuum-dried at 60^{o}C. Data analysis is performed with EDAX Genesis analytical system.

2.5. Tensile test.

We characterize the mechanical properties of lobster membranes using Instron® 3342. Uniaxial tensile measurements are conducted at room temperature in air under a controlled strain rate of 0.017 s^{-1}. Rectangular samples for mechanical tests are cut from a single membrane by scissors. These samples have width from 2 to 5 mm, thickness from 0.3 to 0.5 mm, and length from 10 to 20 mm. To examine the damage tolerance, a notch is introduced onto the rectangular samples by cutting into the multi-layer structure. The notch depth is measured using optical microscopy.

2.6. Structural model of the lobster membrane and mechanical simulations.

We assemble the mechanical model of chitin fibers by explicitly considering the microstructure of lobster membrane to build its structural model. The entire lobster membrane is composed of multiple layers of stacks. We follow the geometry of lobster membrane and build the structure of a mechanical model. This model is used

for molecular dynamics simulations of the mechanical response of the lobster membrane. The entire membrane of 0.3 mm in thickness and 0.1 mm in height and width (see Figure S8 for illustration) is composed of 10 layers of stacks. Each stack is modeled with a height of 30 um (as measured experimentally from the SEM image), which is composed of five characteristic layers with the 36° angle between the neighboring two layers for their fiber angles, according to the measurement from the SEM image. Three sublayers, with the same orientation and close packing for the single layer of chitin fibers (with $2\,\mu m$ in diameter), are included for each characteristic layer in our material model. This model geometry is built by a Matlab program (Mathworks Inc., Natick, US, details in **Figure 1**). We developed a potential function as the mechanical model of chitin fibers and include the damping and viscosity effects of the fibers within the water environment. We run our molecular dynamics simulation by using the Large-scale Atomic/Molecular Massively Parallel Simulator (LAMMPS) package. We first fully relax the simulation model and then apply quasi-static loading to our simulation system by applying the uniaxial strain with 1% increment. Several layers of beads on the lower and upper boundaries of the model are fully constrained to make the model deform as projected (**Supporting Figure S8**). We fully relax the rest parts of the structure after each strain increment and take the measurement of the total stretching force on the boundary as the sum of force on either of the lower or upper boundaries. The strain increment continues until the full rupture of the membrane and we record the full stress-strain data for analysis. The trajectory of all the coarse-grained beads is recorded during the simulation, which is thereafter used to capture the simulation snapshots with VMD and measure the bond length in deformation as well as compute the strain and stress within each fiber by using Matlab.

2.7. A mechanical model of chitin fiber in the lobster membrane.

Each chitin fiber is modeled by a simple bead-spring coarse-grained model with a bead diameter of $d = 2\,\mu m$ and bead distance of $r_0 = 1\,\mu m$. Such small bead distance is intentionally selected to prevent the fiber from penetrating with each other.

The mass of the bead is determined by $m = \pi d^2 r_0 \rho/4$, where ρ is the density of chitin. The total deformation energy of the fibers is defined by

$$E = E_T + E_B + E_{non-bond} \quad (1)$$

where E_T is the axial deformation energy of a fiber's deformation along the axial direction, E_B is the bending energy and $E_{non-bond}$ describes the non-bonded interactions between two beads that are not directly tethered by a spring or angular spring. The E_T term is given by its derivation as the force-displacement curve of each spring, which is composed of three regimes: linear, stiffening and post-peak-stress. The equilibrated spring length is r_0 while the axial force of the spring under deformation to *r* is given by

$$f = \frac{dE_T}{dr} = \begin{cases} k_1(r - r_0) & r < r_1 \\ H(r) & r_1 \le r < r_2 \\ 2D\alpha e^{-\alpha(r-r_{02})}\left[1 - e^{-\alpha(r-r_{02})}\right] & r \ge r_2 \end{cases} \quad (2)$$

And the spring stiffness is given by

$$k = \frac{df}{dr} = \begin{cases} k_1 & r < r_1 \\ H'(r) & r_1 \le r < r_2 \\ 2D\alpha^2 e^{-\alpha(r-r_{02})}\left[2e^{-\alpha(r-r_{02})} - 1\right] & r \ge r_2 \end{cases} \quad (3)$$

It is noted that such function is designed as the combination of spring of harmonic potential energy and spring of Morse potential energy. Here, k_1, *D*, α, r_1, r_2 and r_{02} are all the constants that affect the force-extension curve of the fiber in deformation. According to tensile experiments on the lobster membrane, k_1 as the spring stiffness at equilibrium, has its value 1/15 of the stiffness at the beginning of the stiffening region as $k_2 = 2D\alpha^2 e^{-\alpha(r_2-r_{02})}\left[2e^{-\alpha(r_2-r_{02})} - 1\right]$. $H(r)$ is the Hermite interpolation function that is used to smoothly connect the two curves. The numerical value of r_1, r_2 and r_{02} are obtained from the experimental stress-strain curve of a piece of lobster membrane that defines the boundary of three regimes as $r_1 = 1.2r_0$, $r_2 = 1.75r_0$ and $r_{02} = 1.55r_0$. Other numerical values used for the model include the critical strain of a pristine membrane to reach the peak stress in tension as $\varepsilon_c = 1.8$ is what is measured for an independent tensile test and the

experimental measurement of the chitin fiber strength of $\sigma_{fiber} = 171$ MPa [15, 16], which are used to determine the numerical value of D and α in our model. From Eq. (3), it is noted that to reach the peak force of the fiber, the condition $df/dr = 0$ needs to be satisfied, which leads to $2e^{-\alpha(r-r_{02})} = 1$ and thus we have

$$\alpha = \frac{\log(2)}{r_0(\varepsilon_c+1)-r_{02}} \quad (4)$$

Using Eq. (4) and Eq. (2), it is obtained that $f_{max} = D_0\alpha/2$ is the strength of the chitin fiber. Since $\sigma_{fiber} = 171$ MPa corresponds to the strength of highly crystalline chitin, we include a fitting factor c_1 to consider the defects inside the membrane, as

$$D = c_1\frac{\sigma_{fiber}\pi d^2}{2\alpha} = c_1 D_0 \quad (5)$$

$c_1 \in [0,1]$ is a factor that accounts for the defects at the single fiber level, as $c_1 = 1$ simply means all fibers in the cross-section area are intact and they synergistically contribute to the membrane strength and $c_1 = 0$ means none of the fibers contribute to the membrane strength. The numerical value of $c_1 = 0.19$ is determined by best fitting the simulation results of the stress-strain curve of the pristine membrane with a single experimental tensile test on a lobster membrane as shown in **Figure S7**.

An angular spring between two neighbouring linear springs is inserted to define the bending stiffness of the thread. The bending energy of each angular spring is given by $\varphi_B(\theta) = K_B(\theta - \theta_0)^2$, where θ is the angle between two neighbouring springs and θ_0 is the equilibrium angle. The spring constant K_B is given by

$$K_B = \frac{EI_t}{2r_0} = \frac{k_1 d^2}{32} \quad (6)$$

where $E = 4k_1 r_0/(\pi d^2)$ is the modulus of the fiber at small deformation. The non-bonded interaction is given by a simple Lennard-Jones potential that accounts for both the adhesion force and the repulsion force between fibers, it is defined as

$$E_{non-bond} = 4\epsilon\left[(\frac{\sigma}{r})^{12} - (\frac{\sigma}{r})^{6}\right] \quad (7)$$

where ϵ is the potential energy at equilibrium, and its value is given by $\epsilon = \gamma d r_0$ as γ is the surface energy at the interface between chitin and protein [16]. $\sigma = 2^{-1/6}d$ defines the distance of two non-bonded beads at equilibrium. Damping and viscosity

effects of the fibers within the water environment are included in the model by considering the energy dissipation of each fiber in motion caused by the viscosity of the surrounding water. We note because of the small dimension of the chitin fibers, the Reynolds number is small and the drag force is proportional to the particle velocity. We use the Stokes' law to measure the drag force of a fiber within the water environment by [17]:

$$f_{\text{drag}} = -6\pi\mu R v, \tag{8}$$

where $\mu = 8.6 \times 10^{-4}\ \text{Pa} \cdot \text{s}$ is the fluid viscosity constant of water at room temperature, $R = \sqrt[3]{\frac{3d^2 r_0}{16}}$ is the equivalent spherical radius of the mesoscopic bead, which equals to the radius of a sphere of equivalent volume [18]. The parameter *v* denotes the relative velocity of particle motion in water. The numerical value of all the parameters of the model are included in the **Supporting Table S1**.

2.8 Statistical methods

All quantitative data, except the tensile strength and toughness of lobster membranes, were presented as mean ± standard deviation (error bars). Mean values and standard deviation were calculated using Excel. To obtain the tensile strength and toughness of lobster membranes, we measured samples from more than 10 lobsters. Since different lobsters show wide distribution ranges of tensile strength and toughness, we select medium values to represent the mechanical properties of lobster membranes, rather than unreasonably obtain mean values with error bars.

3. Results and discussion

To investigate the chemical and mechanical properties of the lobster membranes, experimental samples of these membranes are collected from natural lobsters obtained at Boston local fish markets. Membranes at both the abdomen and the joint of lobsters are investigated in our study. These membranes are connected seamlessly to rigid cuticles (**Figure 2a**) and play critical roles for the mobility of lobsters. Interestingly, after removing other tissues connecting to these membranes, they appear to be highly transparent with refractive index close to that of water (**Figures 2b and c**) or

semi-transparent (**Figure 2d**) depending on the tissue location and age and moreover, are extremely flexible, making them easily distinguished from the hard cuticles. It has been revealed that these membranes are mainly made of chitin and proteins[5], which is confirmed by Fourier transform infrared spectroscopy (FTIR) measurements (**Supporting Figure S1**). Interestingly, these membranes have a very high water content (75%~90%), which is 3 times more than that in the cuticles (~28%), as shown in **Figure 2e**. Moreover, these membranes are almost non-mineralized; X-ray photoelectron spectroscopy (XPS) measurements show that the joint and abdomen membranes have a calcium content of 0.36% and 0.18% respectively, which are negligible as compared to the significantly higher content in the cuticles (**Figure 2f)**. Such a small amount of minerals is sparsely distributed, confirmed by energy-dispersive X-ray spectroscopy (EDX) mapping (**Figure 2g**). The high water content and low mineral content correlate with the transparency and flexibility of these materials, suggesting that the lobster membranes are natural hydrogels. However, since typical natural hydrogels are not very mechanically robust[19-22], it is intriguing that how such hydrogel membranes can be a durable part of the lobster exoskeleton and suitable for dynamic and rocky environments.

To gain more insights into the structural and mechanical features of the lobster membranes, we characterize the microstructure of these membranes using scanning electron microscopy (SEM). We find that, instead of having randomly coiled and interconnected polymer chains as observed in typical hydrogels[23-25], the lobster membrane is composed of a multi-layer structure in a lamellar fashion, as shown in the cross-section view of the freeze-dried membrane sample (**Figure 3a**). In each layer, the chitin fibers are highly oriented (**Figure 3b**), and a rotation angle between two neighboring planes is about 36° (**Figure 3b-c**), with a repeated cycle of rotation of 180° (**Figure 3a, inset**). Such a multi-layer structure is universal in both the abdomen membrane and the joint membrane (**Supporting Figure S2**). This structure is also consistent with the twisted plywood structure observed in the lobster cuticle[2, 3] and a variety of hard natural biomaterials[6, 7, 26, 27], suggesting that a similar

chitin-based scaffold may be adopted by both soft and stiff exoskeletons.

To study the mechanical behavior of the hydrogel membranes, we cut rectangular samples and measure their mechanical response by performing the uniaxial tensile test. A typical stress (σ) versus strain (ε) relationship is composed of three regimes, as shown in **Figure 3d (i)**. At a small deformation (ε < 20%), the membrane has a low modulus of ~0.23 MPa that is comparable to many hydrogels[10] and several typical soft biological materials[9, 22]. It becomes significantly stiffer at larger deformations (20% < ε < 110%) with a maximum tangent modulus ($E_{//}$=dσ/dε) more than 100 times greater than the initial modulus; this nonlinear stiffening behavior leads to a high peak stress of ~17.91 MPa at a strain of ~110%. Such a high strength is even comparable to that of natural rubber and rubber composites[28, 29]. Moreover, instead of catastrophic failure found in conventional rubbers and hydrogels (**Supporting Figures S3-5**), the lobster membrane has a significantly delayed rapture and can sustain further stretch up to ~220% strain after the peak stress (**Figure 3d**).

Furthermore, we integrate the σ-ε curve to obtain the strain energy density (U_T) needed to stretch the lobster membrane; we find that U_T increases very quickly with strain during the stiffening process and continues to increase after achieving the peak stress, when the material starts to rupture (**Figure 3d (ii)**). It is noted that due to the limited thickness of lobster membranes, it is difficult to trace the crack tip and measure the energy release rate during fracture. Instead, we quantified the material toughness in terms of toughness modulus as the strain energy density, which represents the ability of a material per unit volume to absorb energy and deform before rupturing. Surprisingly, the toughness U_{Tc}, defined as the maximum U_T upon the final failure, of the lobster membrane is measured to be as high as 14.02 MJ/m^3; such a high toughness, as well as the high strength, make the lobster membrane outperform most of conventional hydrogels [23, 24, 30-32], and even tough hydrogels[23-25] as well as synthetic rubbers[28, 33] as summarized in **Figure 3e**. Only very tough natural rubber and carbon black-rubber composites provide similar performance[28, 29] (**Supporting Figures S4** and **5**). Such high toughness and tensile strength together with such a low initial modulus

provide the basis for the lobster membrane to be extremely flexible at the relaxed state, while become much stiffer to protect from tearing at large deformations. These features make this material multifunctional, which is critical to both the mobility and the survival of the lobster under extreme conditions. Thus, these lobster membranes represent a category of soft yet strong and tough hydrogel materials that cannot be achieved by conventional hydrogels.

To understand how these hydrogel membranes behave with the existence of mechanical damages such as scratches by rocks or predators, we perform uniaxial tensile tests on the lobster membranes with a pre-generated notch across the membranes by cutting into the multi-layer structure, as shown in **Figure 4a**. Such a notch works as a pre-existing crack along the thickness direction from the surface of the membrane and the crack length, measured as the notch depth, is recorded for each sample. We find that the shape of the σ-ε curves and the ductile failure process are not significantly altered by the existence of the notch, as shown in **Figure 4c**. Interestingly, the critical strain at the peak stress of the notched sample is nearly the same as that of the intact sample (**Figure 4c**), while both the tensile strength and the toughness of the notched membrane reduce linearly with the notch depth, as shown in **Figures 4e and 4f**, respectively. These results reveal another critical fact of the lobster membrane: These hydrogel membranes are able to withstand large mechanical deformation of more than 100% strain, and the effective strength of the notched membrane, computed by normalizing the peak stretching force by the residual cross-section area aside from the notched zone, is not affected, despite the presence of a deep notch (**Supporting Figure S6**). Such a feature indicates that the lobster membrane is completely damage-tolerant, making it fundamentally different from conventional hydrogels, rubbers and rubber composites, whose strength and toughness both sharply decrease as soon as a small notch is introduced (**Figures 4e and f**). This damage tolerant behavior is likely to be a result of the multi-layer structure of the membranes. Indeed, in hard and dry materials, laminated structures have been used to enhance the damage tolerance of materials[11, 34-36]; crack

propagation into multi-layers is found to be significantly suppressed as compared to an isotropic material. A key feature of this laminated structure is the weak interaction between adjacent layers; by performing a peeling assay, we indeed find that it only requires a much smaller force to peel off several layers from the rest of the membrane as compared to stretching the membrane, as shown in **Figure 4b**. It is noted that the peeling strength is about 172 N/m as measured. It generates a small force of 0.34 N when peeling a sample of 2 mm in width. If we do a tensile test on the membrane sample of 2 mm in width and 0.5 mm in thickness, the tensile force is about 17.9 N, which is about 50 folds higher than the force used to peel the sample. The comparison suggests that peeling the layers is much easier than breaking the sample along the in-plane directions.

We further utilize a simple computational model with the mesoscopic structure of these membranes to simulate their mechanical behavior[8, 12]. This model is composed of the ordered arrangements of chitin fibers with their geometric features revealed by microscopic structural characterizations and mechanical functions revealed in our tensile tests for the unnotched sample, as well as results in the literature for the strength and interfacial energy of chitin fibers[15, 16] (see Methods and **Supporting Figures S7-9** for details). It is noted that in comparing to the computational model in the former study for fish scale[12], our current model includes the fiber rupture as loading curve of each chitin fiber is composed of three regimes including linear, stiffening and post-peak-stress, as given by Eq. (3). Moreover, our current simulation model includes up to 150 layers of chitin fibers (of 0.3 mm in total) to be similar thickness as the natural lobster membrane (0.2 to 0.6 mm) and contain the pre-existing crack of various length for studying the membrane fracture. We use this membrane model to reproduce the experimental results of the deformation and failure of the notched membranes, and we find good agreements with experiments as summarized in **Figure 4**. Our model reveals that the constituting chitin fibers that are initially curved and not along the stretch direction will be straightened upon stretch, and become aligned toward the stretch direction, resulting in a strain

stiffening behavior; even after rupture, they can still slide apart to further dissipate energy, leading to the significant necking before the final failure (**Figure 4a**). These features also contribute to the flat tails of the σ-ε curves shown in **Figure 4d** and thus the high toughness of this membrane.

Our study further suggests that the unique ordered microstructure of the membrane greatly contributes to its damage tolerance as illustrated in **Figure 5a**, making the lobster membrane much stronger than conventional hydrogels and rubbers. To validate that, we built another material model composed of the same constituting chitin fibers but with the microstructure arranged into a fully randomly coiled form, in analogy to the network structures of conventional hydrogels and rubbers[23]. We repeat the tensile tests on the notched model composed of randomly oriented fibers and map the local deformation of all constituting fibers by measuring the distribution of tensile deformation along each chitin fiber (**Figure 5c**). We find that, for the model with random microstructures, the local deformation only concentrates at the crack tip, as shown in **Figure 5c**. By contrast, the lobster membrane is able to carry the loading force with many layers in the front of the crack. Interestingly, we find that the deformation distribution strongly correlates with the fiber orientation; individual fibers are more deformed in layers with fiber angles close to the stretching direction, as shown in **Figure 5c**. Such a feature makes the lobster membrane different from other typical hydrogels during fracture, as the large, discontinuous cohesive zone is not only located near the crack-tip but includes many ordered layers far from the crack. This feature allows the lobster membrane to dissipate substantially high energy during the crack propagation and leads to the effective strength not affected by the crack length, as shown in experiments in **Supporting Figure S6**. By contrast, many polymer materials with the randomly coiled structure can only dissipate the deformation energy near the crack-tip with a geometry dependent local region of stress concentration; this yields a much weaker material with the existence of cracks, as summarized in **Figure 5b** and **Supporting Figure S9**. Indeed, our simulation results confirm that the material strength reduces significantly as soon as a notch is

generated in the randomly coiled structure, while only slowly reduces in the laminated membrane structure.

4. Conclusions

In summary, we show that the soft membranes from American lobster are natural hydrogels composed of 90% water and a small amount of chitin-protein fibers. These hydrogel membranes have remarkably high strength and toughness which are comparable to natural rubber and carbon-rubber composites, and moreover are damage-tolerant. By combining experiments and simulations, we demonstrate that the exceptional mechanical performance of the lobster membranes highly relies on their unique microstructures, as the multi-layer twisted plywood structure with rotating fibers greatly contribute to their high stretchability and energy dissipation under mechanical loading. Using the large-scale coarse-grained model, we simulate the fracture of lobster membrane and visualize the deformation within each constituting fibers at the crack tip during loading, which cannot be obtained experimentally and is not shown in the former work for other fibrous plywood structures, such as[12]. Our simulation result demonstrates that the lobster membrane is able to carry the loading force with many layers in the front of the crack because of the periodicity of the fiber orientation in front of the crack tip and fibers are more deformed within the entire layers with fiber angles close to the stretching direction. For a membrane composed of fibers with random orientations, in contrast, are more vulnerable to cracks, which significantly reduces the strength, making the material much less defect tolerant. Such a feature makes the lobster membrane different from other typical hydrogels during fracture, as the large, discontinuous cohesive zone is not only located near the crack-tip but includes many ordered layers far from the crack. These advanced mechanical functions are critical for the survival of lobsters in the severe wild environment. Furthermore, the insight we obtain from the lobster indicates that multiple mechanical advantages including flexibility, strength, toughness and damage tolerance, which are usually exclusive for conventional engineering materials [37], can actually be possessed by the same hydrogel membrane material.

This insight would motivate the design of the next generation of multifunctional synthetic soft materials for a variety of applications such as soft body armor with maximized mobility, protection and biocompatibility. Nowadays, most modern body armors sacrifice limb protection to gain mobility, simply because none existing armor materials are flexible enough and they all inhibit movement of the arms and legs. The knowledge learned from the soft membrane of American lobster will shed light on designing a synthetic material that is both tough and flexible, which could eventually enable the armor for full body protection without sacrificing mobility. The material could also have a profound impact in many other engineering applications such as soft robotics, artificial tissues, sealant and delivery vehicles with longevity.

Conflict of Interest

The authors declare no conflict of interest.

Supporting Information

Supporting Information is available online.

Acknowledgment: We thank Hengyi Li for helping experiments on rubber composites, and thank Xuanhe Zhao, Hyunwoo Yuk, and Jiliang Hu for valuable discussions. M. G. would like to acknowledge the support from the Department of Mechanical Engineering at MIT. Z. Q. would like to acknowledge the computing accelerators donated by NVIDIA. This work is supported by National Natural Science Foundation of China (Grant No.: 51673120, to J. W.) and State Key Laboratory of Polymer Materials Engineering (Grant No. sklpme2017-3-05, to J. W.).

Author Contributions: J.W. proposed the study. J. W., M. G. and Z. Q. designed the research. J.W., M.G. and Z.Q. prepared the membrane sample. J.W., F.D., M.G. performed and analyzed most of the mechanical tests. J.W., L.Q., H.Z., M.G. performed the structural characterizations. Z.Q. performed and analyzed the simulation. M.G. coordinated the study. J.W., Z.Q., M.G. wrote the manuscript and all authors revised and approved the manuscript.

REFERENCES

[1] Tshudy D, Donaldson WS, Collom C, Feldmann RM, Schweitzer CE. Hoploparia albertaensis, a new species of clawed lobster (Nephropidae) from the late Coniacian, shallow-marine bad heart formation of northwestern Alberta, Canada. Journal of Paleontology 2005;79:961-8.

[2] Fabritius H, Sachs C, Raabe D, Nikolov S, Friák M, Neugebauer J. Chitin in the exoskeletons of arthropoda: From ancient design to novel materials science. Chitin: Springer; 2011. p. 35-60.

[3] Fabritius HO, Sachs C, Triguero PR, Roobe D. Influence of Structural Principles on the Mechanics of a Biological Fiber-Based Composite Material with Hierarchical Organization: The Exoskeleton of the Lobster Homarus americanus. Adv Mater 2009;21:391-400.

[4] Nikolov S, Petrov M, Lymperakis L, Friák M, Sachs C, Fabritius HO, Raabe D, Neugebauer J. Revealing the design principles of high‐performance biological composites using ab initio and multiscale simulations: the example of lobster cuticle. Advanced Materials 2010;22:519-26.

[5] Andersen SO. Characterization of proteins from arthrodial membranes of the lobster, Homarus americanus. Comparative Biochemistry and Physiology a-Molecular and Integrative Physiology 1998;121:375-83.

[6] Weaver JC, Milliron GW, Miserez A, Evans-Lutterodt K, Herrera S, Gallana I, Mershon WJ, Swanson B, Zavattieri P, DiMasi E, Kisailus D. The Stomatopod Dactyl Club: A Formidable Damage-Tolerant Biological Hammer. Science 2012;336:1275-80.

[7] Yao HM, Dao M, Imholt T, Huang JM, Wheeler K, Bonilla A, Suresh S, Ortiz C. Protection mechanisms of the iron-plated armor of a deep-sea hydrothermal vent gastropod. P Natl Acad Sci USA 2010;107:987-92.

[8] Qin Z, Buehler MJ. Flaw Tolerance of Nuclear Intermediate Filament Lamina under Extreme Mechanical Deformation. Acs Nano 2011;5:3034-42.

[9] Yang W, Sherman VR, Gludovatz B, Schaible E, Stewart P, Ritchie RO, Meyers MA. On the tear resistance of skin. Nature Communications 2015;6.

[10] Li J, Suo Z, Vlassak JJ. Stiff, strong, and tough hydrogels with good chemical stability. J Mater Chem B 2014;2:6708-13.

[11] Gao HJ, Ji BH, Jager IL, Arzt E, Fratzl P. Materials become insensitive to flaws at nanoscale: Lessons from nature. P Natl Acad Sci USA 2003;100:5597-600.

[12] Yang W, Sherman VR, Gludovatz B, Mackey M, Zimmermann EA, Chang EH, Schaible E, Qin Z, Buehler MJ, Ritchie RO, Meyers MA. Protective role of Arapaima gigas fish scales: Structure and mechanical behavior. Acta Biomater 2014;10:3599-614.

[13] Shin YA, Yin S, Li XY, Lee SB, Moon SM, Jeong JW, Kwon M, Yoo SJ, Kim YMK, Zhang T, Gao H, Oh SH. Nanotwin-governed toughening mechanism in hierarchically structured biological materials. Nature Communications 2016;7.

[14] Qin Z, Gautieri A, Nair AK, Inbar H, Buehler MJ. Thickness of Hydroxyapatite Nanocrystal Controls Mechanical Properties of the Collagen-Hydroxyapatite Interface. Langmuir 2012;28:1982-92.

[15] Nishino T, Matsui R, Nakamae K. Elastic modulus of the crystalline regions of chitin and chitosan. Journal of Polymer Science Part B-Polymer Physics 1999;37:1191-6.

[16] Jin K, Feng X, Xu Z. Mechanical Properties of Chitin-Protein Interfaces: A Molecular Dynamics Study. BioNanoScience 2013;3:312-20.

[17] Batchelor GK. An introduction to fluid dynamics. 1st Cambridge Mathematical Library ed. Cambridge, U.K. ; New York, NY: Cambridge University Press; 2000.

[18] Jennings BR, Parslow K. Particle-Size Measurement - the Equivalent Spherical Diameter.

Proceedings of the Royal Society of London Series a-Mathematical Physical and Engineering Sciences 1988;419:137-49.
[19] Drury JL, Dennis RG, Mooney DJ. The tensile properties of alginate hydrogels. Biomaterials 2004;25:3187-99.
[20] Wang X, Wang H, Brown HR. Jellyfish gel and its hybrid hydrogels with high mechanical strength. Soft Matter 2011;7:211-9.
[21] Simha NK, Carlson CS, Lewis JL. Evaluation of fracture toughness of cartilage by micropenetration. Journal of Materials Science: Materials in Medicine 2004;15:631-9.
[22] Ashby MF, Gibson LJ, Wegst U, Olive R. The mechanical properties of natural materials. I. Material property charts. Proc R Soc Lond A 1995;450:123-40.
[23] Sun J-Y, Zhao XH, Illeperuma WR, Chaudhuri O, Oh KH, Mooney DJ, Vlassak JJ, Suo Z. Highly stretchable and tough hydrogels. Nature 2012;489:133-6.
[24] Gong JP, Katsuyama Y, Kurokawa T, Osada Y. Double‐Network Hydrogels with Extremely High Mechanical Strength. Adv Mater 2003;15:1155-8.
[25] Sun TL, Kurokawa T, Kuroda S, Ihsan AB, Akasaki T, Sato K, Haque MA, Nakajima T, Gong JP. Physical hydrogels composed of polyampholytes demonstrate high toughness and viscoelasticity. Nat Mater 2013;12:932-7.
[26] Patek SN, Korff WL, Caldwell RL. Biomechanics: Deadly strike mechanism of a mantis shrimp. Nature 2004;428:819-20.
[27] Zimmermann EA, Gludovatz B, Schaible E, Dave NKN, Yang W, Meyers MA, Ritchie RO. Mechanical adaptability of the Bouligand-type structure in natural dermal armour. Nature communications 2013;4:2634.
[28] Xing W, Tang MZ, Wu JR, Huang GS, Li H, Lei ZY, Fu X, Li HY. Multifunctional properties of graphene/rubber nanocomposites fabricated by a modified latex compounding method. Compos Sci Tech 2014;99:67-74.
[29] Li HY, Yang L, Weng GS, Xing W, Wu JR, Huang GS. Toughening rubbers with a hybrid filler network of graphene and carbon nanotubes. J Mater Chem A 2015;3:22385-92.
[30] Gaharwar AK, Rivera CP, Wu C-J, Schmidt G. Transparent, elastomeric and tough hydrogels from poly(ethylene glycol) and silicate nanoparticles. Acta Biomaterialia 2011;7:4139-48.
[31] Nakayama A, Kakugo A, Gong JP, Osada Y, Takai M, Erata T, Kawano S. High Mechanical Strength Double-Network Hydrogel with Bacterial Cellulose. Advanced Functional Materials 2004;14:1124-8.
[32] Xing Q, Yates K, Vogt C, Qian Z, Frost MC, Zhao F. Increasing Mechanical Strength of Gelatin Hydrogels by Divalent Metal Ion Removal. Scientific Reports 2014;4:4706.
[33] Thomas S, Stephen R. Rubber Nanocomposites: Preparation, Properties, and Applications. Singapore: John Wiley & Sons; 2010.
[34] Li L, Ortiz C. A Natural 3D Interconnected Laminated Composite with Enhanced Damage Resistance. Advanced Functional Materials 2015;25:3463-71.
[35] Miserez A, Weaver JC, Thurner PJ, Aizenberg J, Dauphin Y, Fratzl P, Morse DE, Zok FW. Effects of Laminate Architecture on Fracture Resistance of Sponge Biosilica: Lessons from Nature. Advanced Functional Materials 2008;18:1241-8.
[36] Mirzaeifar R, Dimas LS, Qin Z, Buehler MJ. Defect-Tolerant Bioinspired Hierarchical Composites: Simulation and Experiment. ACS Biomaterials Science & Engineering 2015;1:295-304.
[37] Ritchie RO. The conflicts between strength and toughness. Nat Mater 2011;10:817-22.

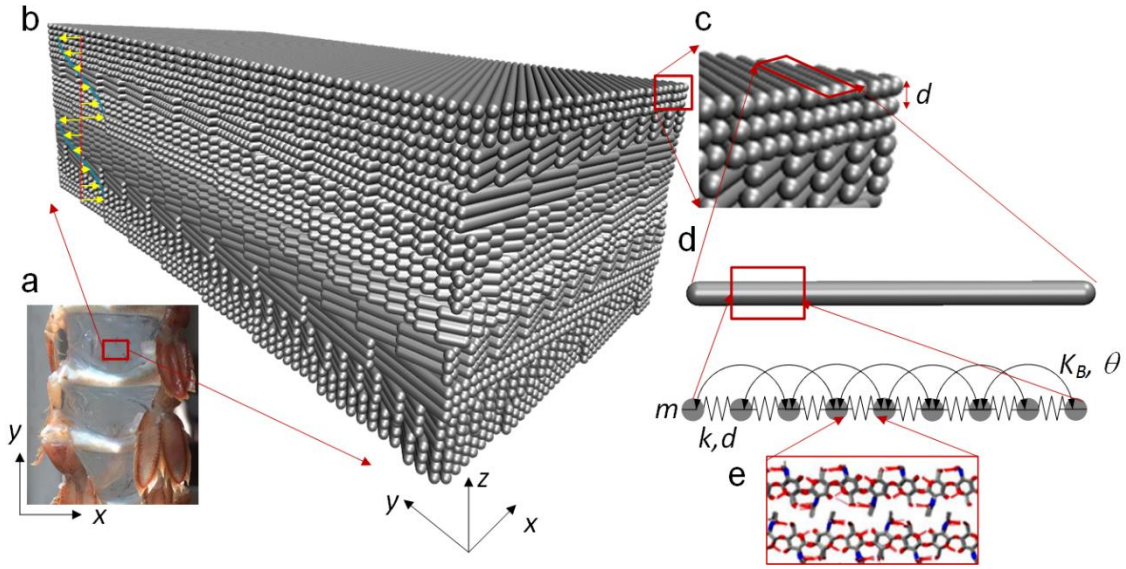

Figure 1. The multiscale structural insight of the lobster membrane that is included in our simulation model: from macroscopic lobster scale to nanoscopic molecular scale. These figures include **(a)** lobster abdomen (at cm scale). **(b)** lobster membrane model (at mm scale) of 2 layers of stacks, with yellow arrows pointing at the normal direction of the chitin fibers, giving the same periodic structure as seen in experiments; **(c)** assembly of layers (at 10 μm scale). **(d)** assembly of chitin fibers (at μm scale), which is the basic unit in our mesoscopic model and is composed of mass beads connected by nonlinear springs bonding between two neighboring beads and angular springs between two neighboring bonds. **(e)** molecular structure of α-chitin crystal, which provides the basic mechanical properties that are used to parameterize the springs in the chitin fiber model.

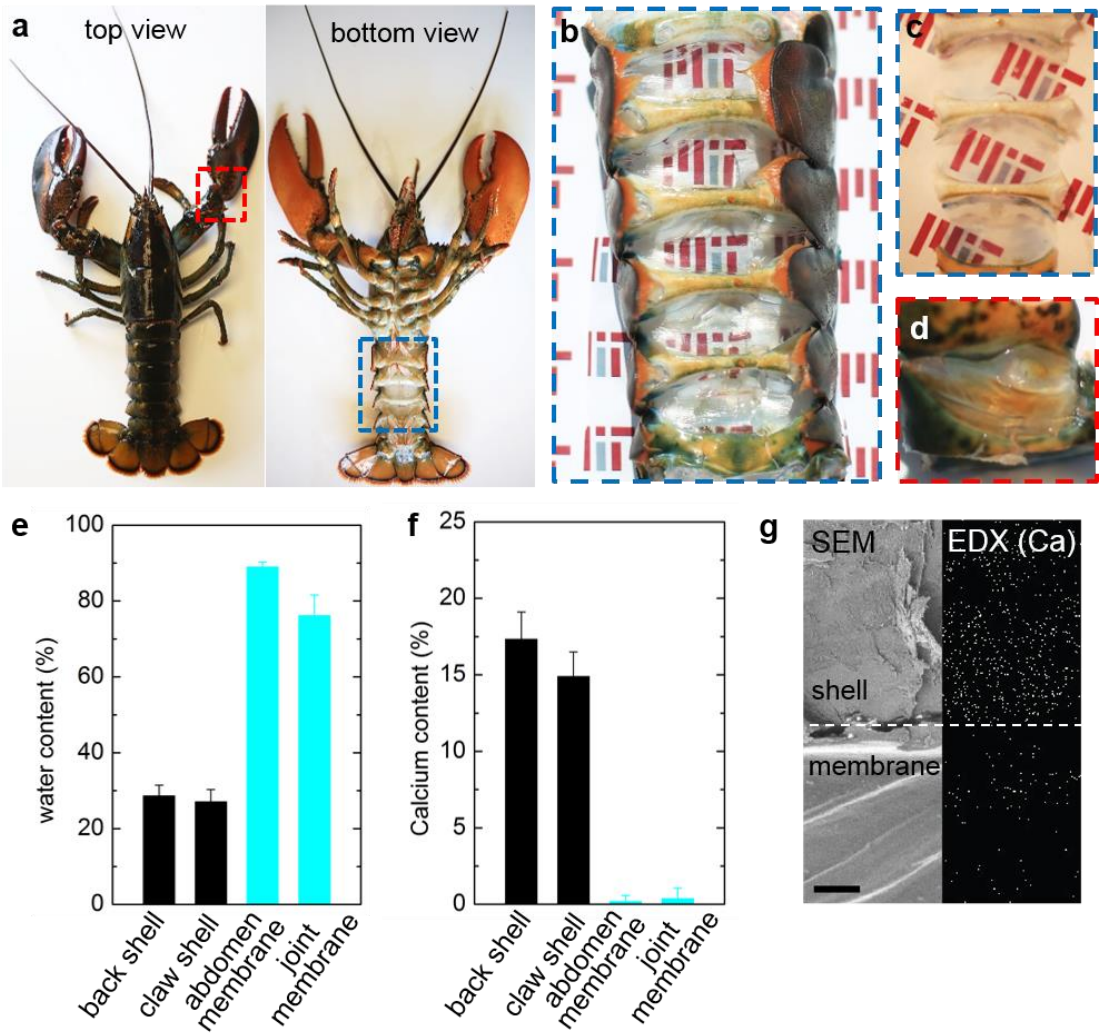

Figure 2. The structural and chemical features of lobster membranes. (a) Top view and bottom view of an American lobster with its soft membranes highlighted by blue (abdomen membrane) and red (joint membrane) boxes. **(b, c)** The abdomen membrane is highly transparent after removing other tissues, both in air **(b)** and under seawater **(c)**. **(d)** The joint membrane is flexible and enables the movement of the lobster. **(e, f)** The lobster membranes have a much higher water content **(e)** and a much lower calcium content **(f)** than hard cuticle materials as measured by weighing dried and naturally hydrated samples and by XPS tests, suggesting the lobster membranes are hydrogels. **(g)** SEM images together with EDX analysis show the difference of the calcium distribution within the hard cuticle and the soft membrane. Scale bar: 100μm

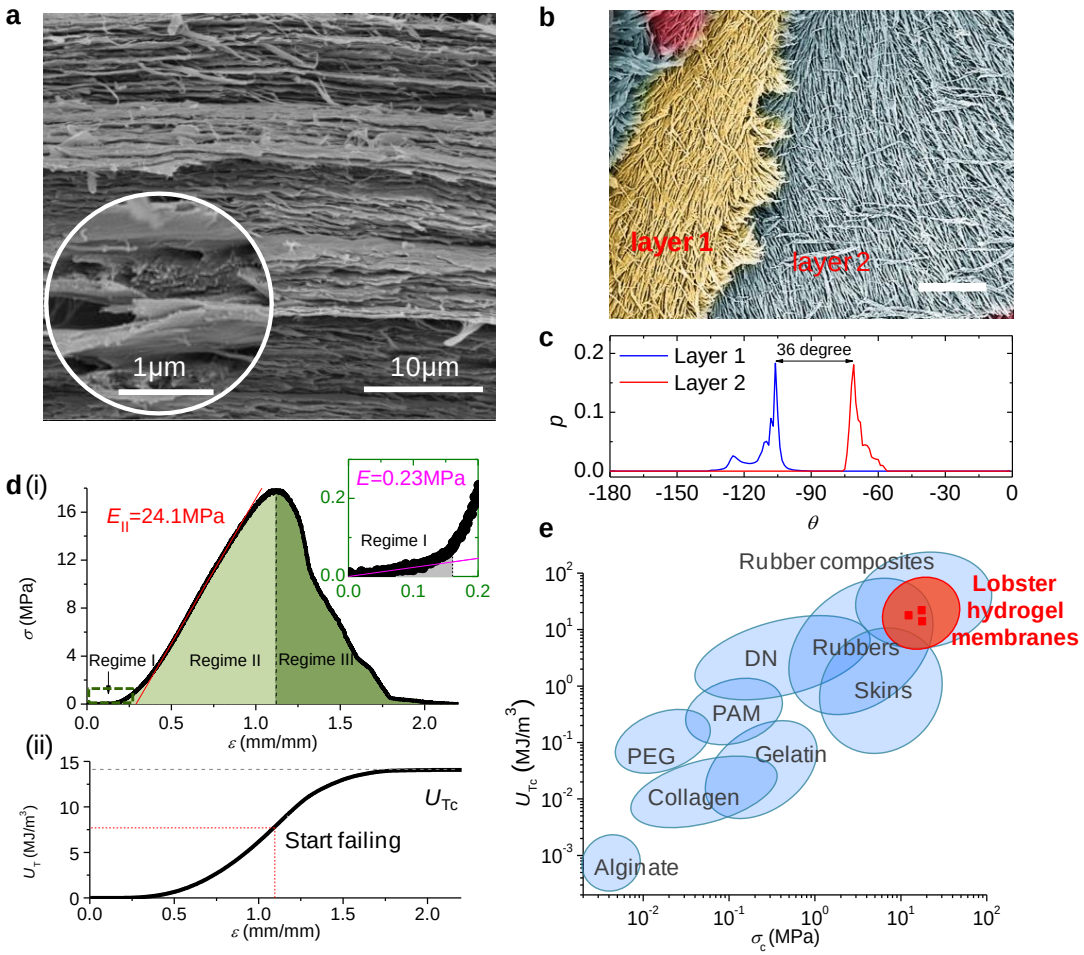

Figure 3. The microscopic structural and mechanical properties of lobster membranes. (a) Cross-section SEM image taken for the multi-layer plywood structure of a freeze-dried lobster membrane. The inset is a zoomed-in view of the cross section with a magnification of 50000, showing the detail of the constituting layers and fibers within the membrane. **(b)** Top view of the lobster membrane at the fracture edge, showing that the layers comprise of fibers, scale bar: 50μm. Pseudocolor is applied to each layer to increase the contrast between neighboring layers. **(c)** The distribution of the orienting directions of the constituting fibers in the two neighboring layers. **(d)** The stress (σ) and strain energy density (U_T) as functions of strain (ε) of a lobster membrane sample from a uniaxial tensile test are shown in panel (i) and panel (ii), respectively. **(e)** The material toughness (U_{Tc}) and tensile strength (σ_c) of lobster membranes in comparison to other typical soft materials. Data for alginate hydrogels (alginate), collagen hydrogels (collagen), gelatin hydrogels (gelatin), poly(ethylene glycol) hydrogels (PEG), polyacrylamide hydrogels (PAM), double network hydrogels (DN), animal skins (skins), rubbers and rubber composites are extracted from **Supporting Figures S3-5 and Supporting references S1-16**.

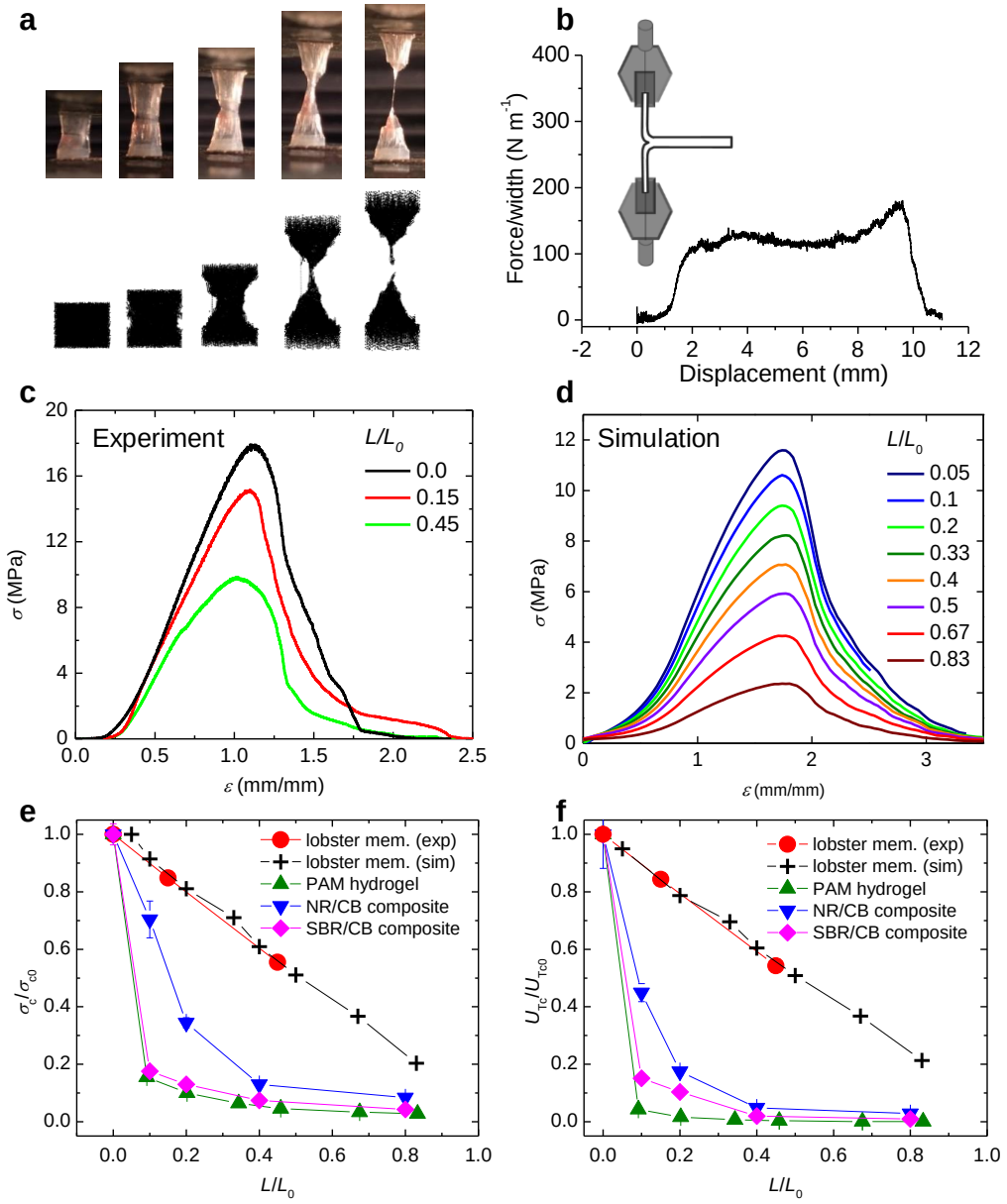

Figure 4. The deformation and failure behaviors of lobster membranes with a notch. (a) Snapshots taken from the experiment (upper) and simulation (lower) of a notched membrane sample during tensile tests. **(b)** The force-displacement curve obtained during peeling a few layers of a membrane sample from the rest; inset shows a schematic of the experimental setup. **(c, d)** σ-ε curves for notched membrane samples of different notch depths (given by L/L_0, with L_0 the total thickness of the membrane and L the thickness of the notched zone) that are obtained from experiments (c) and simulations (d). **(e, f)** The normalized toughness (U_{Tc}/U_{Tc0}) (e) and strength (σ_c/σ_{c0}) (f) of the notched membrane samples with different notch depths, in comparison with other hydrogel and composite materials. Exp and sim in (e, f) represent experimental data obtained by tensile tests and simulation data extracted from the computational model, respectively.

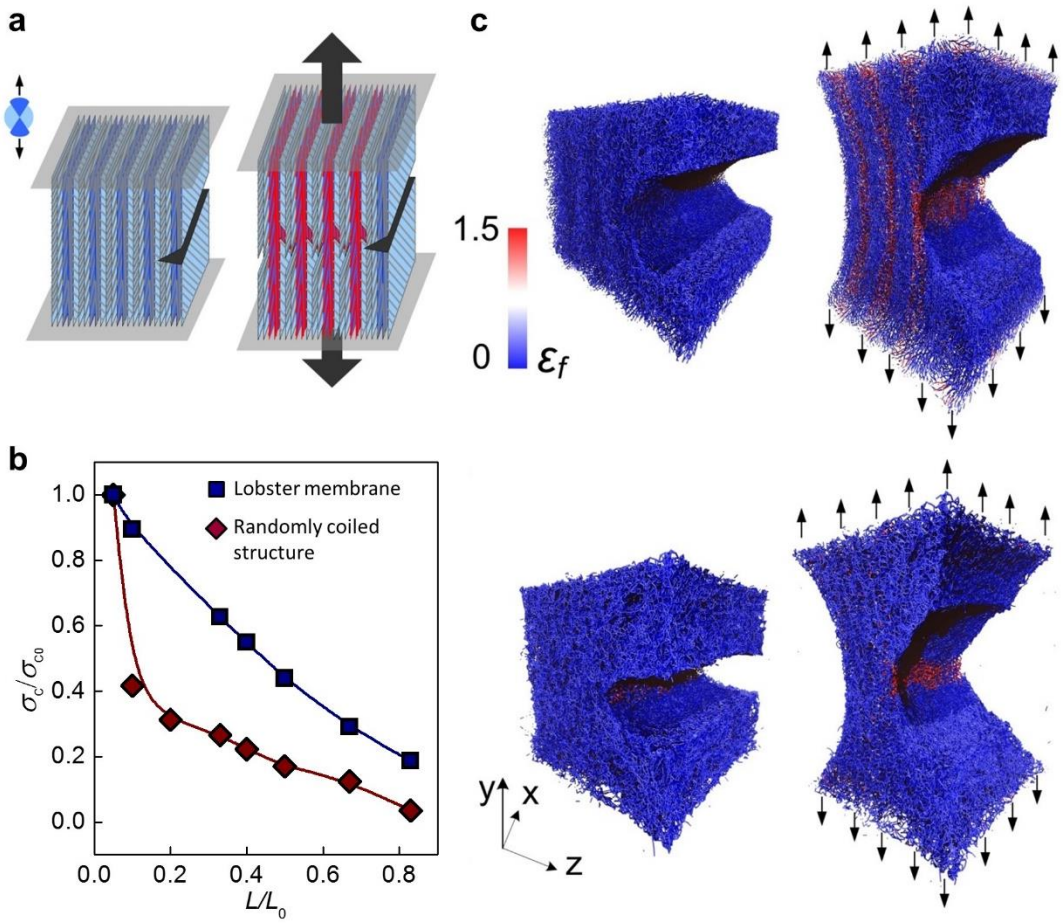

Figure 5. Simulation of the lobster membrane model under loading. (a) Schematic illustration of the deformation and failure process of the notched lobster membrane. The membrane layers take the plywood structure and each of these layers is colored according to the orientation of the comprising chitin fibers (darker color for the orientation ±30° with the loading direction). The layers with fibers oriented close to the loading direction at the front of the notch synergistically contribute to the strength to yield high strength and toughness. **(b)** The normalized lobster membrane strength (defined as σ_c/σ_{c0} where σ_c are peak stress shown in **Fig. 3d**) in comparison with that of a fully randomly coiled microstructure, in analogy to the network structures of conventional hydrogels and rubbers. **(c)** Simulation snapshots of the lobster membrane (top) and the randomly coiled model (bottom) around the notch tip, taken at a small deformation (left) near the initial state and at a large deformation (right) before rupture. Each fiber section is colored according to the strain of individual fiber as measured during the simulation.